All-fiber mode-locked laser oscillator with pulse energy of 34 nJ using a single-walled carbon nanotube saturable absorber

Hwanseong Jeong,[1] Sun Young Choi,[1] Fabian Rotermund,[1] Yong-Ho Cha,[2] Do-Young Jeong,[2] and Dong-Il Yeom[1,*]

[1]*Department of Physics and Department of Energy Systems Research, Ajou University, Suwon, Gyeonggi 443-749, South Korea*

[2]*Quantum Optics Division, Korea Atomic Energy Research Institute, Daejeon 305-600, South Korea*

[*]*diyeom@ajou.ac.kr*

Abstract: We demonstrate a dissipative soliton fiber laser with high pulse energy (>30 nJ) based on a single-walled carbon nanotube saturable absorber (SWCNT-SA). In-line SA that evanescently interacts with the high quality SWCNT/polymer composite film was fabricated under optimized conditions, increasing the damage threshold of the saturation fluence of the SA to 97 mJ/cm^2. An Er-doped mode-locked all-fiber laser operating at net normal intra-cavity dispersion was built including the fabricated in-line SA. The laser stably delivers linearly chirped pulses with a pulse duration of 12.7 ps, and exhibits a spectral bandwidth of 12.1 nm at the central wavelength of 1563 nm. Average power of the laser output is measured as 335 mW at an applied pump power of 1.27 W. The corresponding pulse energy is estimated to be 34 nJ at the fundamental repetition rate of 9.80 MHz; this is the highest value, to our knowledge, reported in all-fiber Er-doped mode-locked laser using an SWCNT-SA.

OCIS codes: (060.3510) Lasers, fiber; (140.4050) Mode-locked lasers; (160.4330) Nonlinear optical materials.

References and links

1. M. E. Fermann and I. Hartl, "Ultrafast Fiber Laser Technology," IEEE J. Sel. Top. Quantum Electron. **15**(1), 191–206 (2009).
2. R. R. Gattass and E. Mazur, "Femtosecond laser micromachining in transparent materials," Nat. Photonics **2**(4), 219–225 (2008).
3. C. L. Hoy, O. Ferhanoglu, M. Yildirim, K. Ki Hyun, S. S. Karajanagi, K. M. C. Chan, J. B. Kobler, S. M. Zeitels, and A. Ben-Yakar, "Clinical Ultrafast Laser Surgery: Recent Advances and Future Directions," IEEE J. Sel. Top. Quantum Electron. **20**(2), 242–255 (2014).
4. C. Xu and F. W. Wise, "Recent advances in fibre lasers for nonlinear microscopy," Nat. Photonics **7**(11), 875–882 (2013).
5. V. J. Matsas, T. P. Newson, D. J. Richardson, and D. N. Payne, "Selfstarting passively mode-locked fibre ring soliton laser exploiting nonlinear polarisation rotation," Electron. Lett. **28**(15), 1391–1393 (1992).
6. U. Keller, K. J. Weingarten, F. X. Kartner, D. Kopf, B. Braun, I. D. Jung, R. Fluck, C. Honninger, N. Matuschek, and J. Aus der Au, "Semiconductor saturable absorber mirrors (SESAM's) for femtosecond to nanosecond pulse generation in solid-state lasers," IEEE J. Sel. Top. Quantum Electron. **2**(3), 435–453 (1996).
7. S. Y. Set, H. Yaguchi, Y. Tanaka, and M. Jablonski, "Ultrafast fiber pulsed lasers incorporating carbon nanotubes," IEEE J. Sel. Top. Quantum Electron. **10**(1), 137–146 (2004).
8. W. B. Cho, J. H. Yim, S. Y. Choi, S. Lee, U. Griebner, V. Petrov, and F. Rotermund, "Mode-locked self-starting Cr:forsterite laser using a single-walled carbon nanotube saturable absorber," Opt. Lett. **33**(21), 2449–2451 (2008).
9. Q. Bao, H. Zhang, Y. Wang, Z. Ni, Y. Yan, Z. X. Shen, K. P. Loh, and D. Y. Tang, "Atomic-layer graphene as a saturable absorber for ultrafast pulsed lasers," Adv. Funct. Mater. **19**(19), 3077–3083 (2009).
10. Z. Sun, T. Hasan, F. Torrisi, D. Popa, G. Privitera, F. Wang, F. Bonaccorso, D. M. Basko, and A. C. Ferrari, "Graphene mode-locked ultrafast laser," ACS Nano **4**(2), 803–810 (2010).
11. F. Bonaccorso and Z. Sun, "Solution processing of graphene, topological insulators and other 2d crystals for ultrafast photonics," Opt. Mater. Express **4**(1), 63–78 (2014).

#217567 - $15.00 USD Received 22 Jul 2014; revised 6 Sep 2014; accepted 8 Sep 2014; published 11 Sep 2014

12. S. Kivistö, T. Hakulinen, A. Kaskela, B. Aitchison, D. P. Brown, A. G. Nasibulin, E. I. Kauppinen, A. Härkönen, and O. G. Okhotnikov, "Carbon nanotube films for ultrafast broadband technology," Opt. Express **17**(4), 2358–2363 (2009).
13. W. B. Cho, J. H. Yim, S. Y. Choi, S. Lee, A. Schmidt, G. Steinmeyer, U. Griebner, V. Petrov, D.-I. Yeom, K. Kim, and F. Rotermund, "Boosting the nonlinear optical response of carbon nanotube saturable absorbers for broadband mode-locking of bulk lasers," Adv. Funct. Mater. **20**(12), 1937–1943 (2010).
14. B. Fu, Y. Hua, X. Xiao, H. Zhu, Z. Sun, and C. Yang, "Broadband graphene saturable absorber for pulsed fiber lasers at 1, 1.5, and 2 mm," IEEE J. Sel. Top. Quantum Electron. **20**(5), 1100705 (2014).
15. K. Kieu and M. Mansuripur, "Femtosecond laser pulse generation with a fiber taper embedded in carbon nanotube/polymer composite," Opt. Lett. **32**(15), 2242–2244 (2007).
16. Y.-W. Song, S. Yamashita, C. S. Goh, and S. Y. Set, "Carbon nanotube mode lockers with enhanced nonlinearity via evanescent field interaction in D-shaped fibers," Opt. Lett. **32**(2), 148–150 (2007).
17. J. H. Im, S. Y. Choi, F. Rotermund, and D.-I. Yeom, "All-fiber Er-doped dissipative soliton laser based on evanescent field interaction with carbon nanotube saturable absorber," Opt. Express **18**(21), 22141–22146 (2010).
18. H. Jeong, S. Y. Choi, E. I. Jeong, S. J. Cha, F. Rotermund, and D.-I. Yeom, "Ultrafast mode-locked fiber laser using a waveguide-type saturable absorber based on single-walled carbon nanotubes," Appl. Phys. Express **6**(5), 052705 (2013).
19. S. Y. Choi, F. Rotermund, H. Jung, K. Oh, and D.-I. Yeom, "Femtosecond mode-locked fiber laser employing a hollow optical fiber filled with carbon nanotube dispersion as saturable absorber," Opt. Express **17**(24), 21788–21793 (2009).
20. S. Y. Choi, H. Jeong, B. H. Hong, F. Rotermund, and D.-I. Yeom, "All-fiber dissipative soliton laser with 10.2 nJ pulse energy using an evanescent field interaction with graphene saturable absorber," Laser Phys. Lett. **11**(1), 015101 (2014).
21. S. Y. Ryu, K.-S. Kim, J. Kim, and S. Kim, "Degradation of optical properties of a film-type single-wall carbon nanotubes saturable absorber (SWNT-SA) with an Er-doped all-fiber laser," Opt. Express **20**(12), 12966–12974 (2012).
22. H. Jeong, S. Y. Choi, F. Rotermund, and D.-I. Yeom, "Pulse width shaping of passively mode-locked soliton fiber laser via polarization control in carbon nanotube saturable absorber," Opt. Express **21**(22), 27011–27016 (2013).

1. Introduction

Passively mode-locked all-fiber lasers generating ultra-short optical pulses have been intensively studied with their merits including alignment-free structure, excellent spatial beam profile, and compactness [1]. These can be potentially applicable for micro-machining, micro-surgery, and bio-imaging [2–4]. In a passively mode-locked fiber laser, saturable absorbers (SAs), i.e., optical components exhibiting a nonlinear response of optical absorption to the incident optical intensity, are necessarily used for initiating and stabilizing the pulsed laser operation. Although passive mode-locking can be realized through artificial means such as additive pulse mode-locking or nonlinear polarization evolution (NPE) [5] in the fiber lasers, saturable absorption elements such as semiconductor saturable absorber mirrors (SESAMs) [6] are popularly employed for environmentally robust and stable laser mode-locking. Recently, novel SAs based on low-dimensional materials including single-walled carbon nanotube (SWCNT), graphene and topological insulators have drawn great attention as an alternative to the SESAM [7–11] In particular low-dimensional carbon materials exhibit advantages such as broadband operation range covering the near IR to mid-IR wavelengths, fast nonlinear response time, and relatively simple fabrication process. In the last decade, passive mode-locking based on carbon-based SAs has been successfully applied in both bulk solid-state and fiber laser systems at broad spectral ranges [12–14].

Since carbon nanomaterials are relatively easy to integrate into optical systems compared to SESAMs, there have been several attempts to make efficient interactions with light in the SAs for fiber lasers. Whereas direct interaction by coating the SA on the fiber ferrule end is simple and convenient, its limited nonlinear interaction length and optically induced thermal damages can be obstacles for scaling up the pulse energy of the fiber lasers. A promising alternative for solving these issues is through lateral interaction with evanescent waves. Indeed, SAs employing evanescent wave interaction have been proposed on the basis of several platforms including tapered fibers [15], side-polished fibers [16, 17], planar lightwave circuits [18], and hollow optical fibers [19]. Among the suggested platforms, the SA on the

#217567 - $15.00 USD Received 22 Jul 2014; revised 6 Sep 2014; accepted 8 Sep 2014; published 11 Sep 2014

side-polished fiber (SPF) holds advantages such as robust and large nonlinear interaction length (~few mm), compatibility with conventional single-mode fibers, and reduced optical power in the interaction region, which will be beneficial for high-power operation of fiber lasers. Although there have been previous researches on all-fiber mode-locked lasers with high pulse energy using an SWCNT- or graphene-SAs on an SPF [17, 20], large absorption loss with a strong polarization dependence of the SA limits the fiber laser output power (174 mW) and the pulse energy (~10 nJ).

In our present work, we optimized SWCNT-SA fabrication for high-power operation of the fiber laser. A uniformly dispersed high-quality SWCNT/PMMA film was spin-coated on the prepared SPF, which exhibited a low insertion loss (– 1.32 dB) with a moderate polarization-dependent loss (PDL) of 5.56 dB. The optical properties of the fabricated SA were analyzed through nonlinear transmission measurement. Using our SA, an all-fiber dissipative soliton fiber laser oscillator was built that operates at net normal cavity dispersion. The fabricated all-fiber laser stably delivered linearly chirped pulses of 12.7 ps, which were compressed to 369 fs using an additional fiber delay at the laser output. The laser output power was measured as 335 mW and the corresponding pulse energy was 34 nJ at the fundamental repetition rate of 9.80 MHz. In addition, we investigated the optical damage threshold of the SWCNT-SA on an SPF for the first time. We observed that defects were developed above a saturation fluence energy of 97 mJ/cm^2, which is a much higher threshold than reported value (~100 μJ/cm^2) [21] in the SWCNT-SA on fiber ferrules.

2. Fabrication and characteristic analysis of the SWCNT-SA

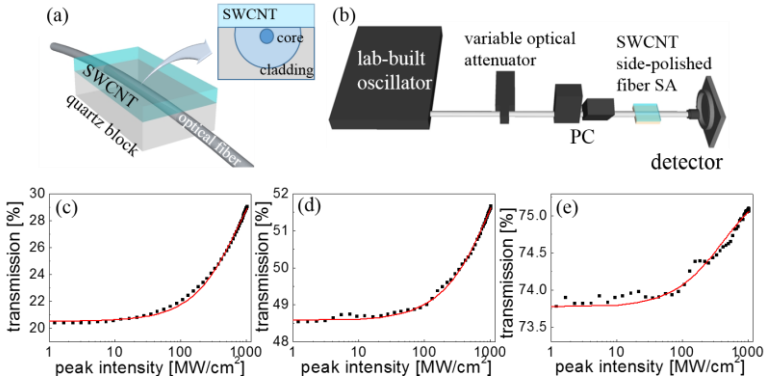

Fig. 1. (a) Schematic image of the SWCNT-SA on the SPF (inset: cross-sectional view of SWCNT-SA structure), (b) experimental set-up for nonlinear transmission measurement of the SA, (c)-(e) nonlinear transmission results of (c) TE-mode, (d) intermediate, and (e) TM-mode polarization states.

A commercial SWCNT synthesized through the high-pressure CO conversion (HiPCO) method was dispersed via ultrasonic agitation and mixed with poly(methyl methacrylate) (PMMA) solution where detailed description of fabrication process can be found in Ref. 13 and Ref. 19. The SWCNT/PMMA composite exhibits broadband absorption around 1550 nm [13], which corresponds to the E_{11} transition of semiconducting SWCNTs. The composite was then spin-coated on side-polished fiber (SPF). Figure 1(a) shows a schematic image of a fabricated SWCNT-SA on an SPF. In the fabrication process of the SPF, we optimally set the index-oil drop loss to – 25 dB where the closest distance between fiber core boundary and polished surface, and the interaction length of the SPF were estimated to be about 1.5 μm and 2 mm, respectively. The SPF initially exhibits a fiber-to-fiber insertion loss of – 0.1 dB with a negligible PDL. The performance of the SPFs was quite reliable during repeated fabrications. As increasing the number of spin-coating processes of the SWCNT, the insertion loss and PDL of the devices varies with oscillating behavior [17]. The modulation depth of the SA can

#217567 - $15.00 USD Received 22 Jul 2014; revised 6 Sep 2014; accepted 8 Sep 2014; published 11 Sep 2014

be increased at high PDL of the devices, but it causes large absorption leading to optical damage of the SA at high power. After five times controlled spin-coating processes, we obtained the SWCNT-SA possessing a relatively small insertion loss of – 1.32 dB with a moderate PDL of – 5.56 dB, which can be compared to those of – 4.6 dB and – 15.3 dB reported in Ref. 17. A thickness of the SWCNT/PMMA composite film is estimated to be about 3.8 μm. We then performed a nonlinear transmission measurement using the system depicted in Fig. 1(b). A lab-built mode-locked fiber laser was used for the nonlinear measurement along with a motor driven variable attenuator and a photo-detector. The pulse width (400 fs) of the laser was measured after propagating the same length of the fiber with that of our in-line SA to precisely estimate the pulse peak power at the SA. The state of polarization of the incident light was managed by a polarization controller (PC). Figures 1(c)-1(e) show the results of the nonlinear transmission measurement for several input polarization states. In the transverse electric (TE) mode, in which the polarization direction is parallel to the polished surface of the SPF, the initial linear transmission of 20.5% increases up to 29%, as shown in Fig. 1(c). The nonlinear transmission of the intermediate polarization state shows an initial linear loss of 48.6%, which increases to 51.6% at maximum power output of the laser (Fig. 1(d)). For the transverse magnetic (TM) input polarization, the nonlinear transmission of 73.7% at low power increases to 75.1% at maximum power output (Fig. 1(e)). Although the fully saturated value was not achieved in the nonlinear transmission measurement because of the limited power of the current system, we expect that the SA properties, including the modulation depth and the non-saturable loss, can be controlled by adjusting the intra-cavity polarization state of the laser [22].

3. Fiber laser experiment using an SWCNT-SA

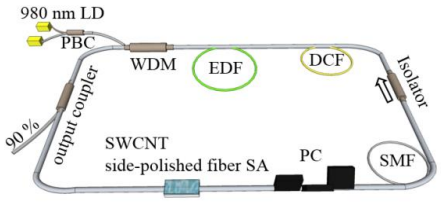

Fig. 2. Configuration of the constructed all-fiber ring laser using an SWCNT-SA.

Figure 2 depicts the schematic of the fabricated all-fiber fiber laser oscillator with our SWCNT-SA. A heavily Er-doped fiber (Er80-8/125, Liekki^{TM}, β_2 ~– 22.3 ps^2/km) with a length of 1.4 m was pumped by core-pumped laser diodes (LDs) via a wavelength division multiplexing (WDM) coupler. Here, we employed a polarization beam combiner (PBC) to increase pump power up to 1.4 W. A dispersion compensating fiber (DCF) with a length of 3.4 m and a dispersion of 162 ps^2/km and extra SMF-28e fiber were used for managing the cavity dispersion of the laser. A polarization controller (PC) was added for intra-cavity polarization control and an isolator was inserted to ensure unidirectional operation of the laser. The fabricated SA was then applied to the laser cavity. Stable passive mode-locking of a dissipative soliton laser was obtained at a net cavity dispersion of around 0.141 ps^2, where total length of the laser cavity including an SMF-28e (15.6 m) and an HI1060 (0.7 m) is estimated to be approximately 21.1 m.

We explored laser output characteristics of the dissipative soliton fiber laser for several different output couplers. Figure 3 compares the mode-locking (ML) threshold and average output power of the laser for a given pump power. The stable ML started from a pump power of 105 mW when we used a 5:5 output coupler. The ML threshold increased to 181 mW and 304 mW for 8:2 and 9:1 output couplers respectively. The laser output power also increased when we used directional couplers with a higher output coupling ratio, as shown in Fig. 3. The mode-locked operation became unstable when the 95:5 output coupler was employed.

#217567 - $15.00 USD Received 22 Jul 2014; revised 6 Sep 2014; accepted 8 Sep 2014; published 11 Sep 2014

Thus, we obtained the maximum laser output power with the 9:1 output coupler, where the maximum average output power of 335 mW was measured at the applied pump power of 1.27 W. We experimentally confirm that the laser operation is stably maintained for 24 hours. As we further increased the pump power up to maximum value of 1.4W, stable but multi-pulsing operation per round trip of the laser cavity was observed where the measured average output power was 380 mW.

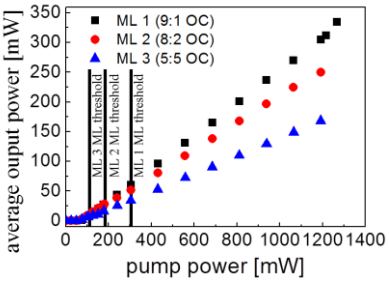

Fig. 3. Comparison of average output power and ML threshold of the mode-locked fiber laser using an SWCNT-SA with various output couplers.

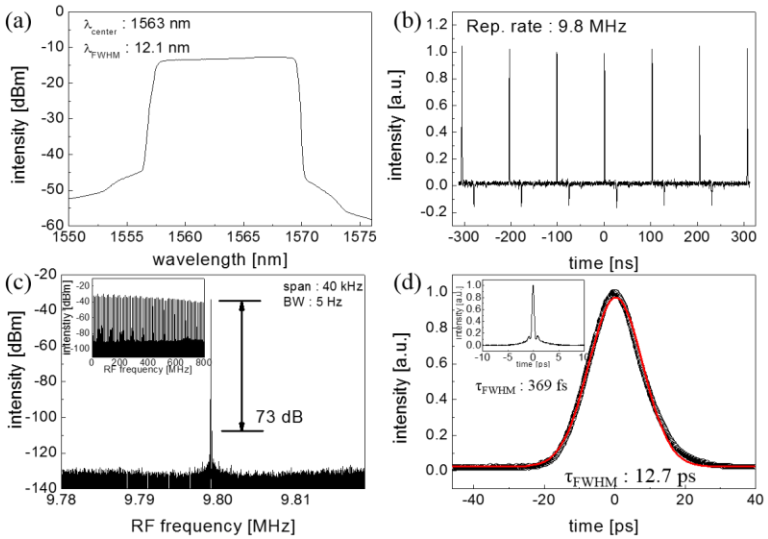

Fig. 4. Laser output characteristics of the fabricated dissipative soliton fiber laser with 9:1 output coupler: (a) optical spectrum, (b) pulse train, (c) RF-spectrum (inset: RF spectrum with large span range), and (d) auto-correlation trace (inset: auto-correlation trace after compression).

Figure 4 shows the laser output characteristics of the dissipative soliton fiber laser using a 9:1 output coupler. The spectral bandwidth of the laser was measured to be 12.1 nm at the central wavelength of 1563 nm, as shown in Fig. 4(a). The repetition rate of the laser output pulse train was 9.80 MHz (Fig. 4(b)), which corresponds to a laser cavity length of 21.1 m. From the measured average output power of 335 mW, the pulse energy was estimated as 34 nJ, which is the largest value, to our knowledge, reported for an all-fiber dissipative soliton fiber laser using an SWCNT-SA. Figure 4(c) displays the RF spectrum of the laser pulse train. The signal-to-noise ratio of 73 dB from the fundamental repetition rate and its harmonics (inset) over a broad range indicates stable mode-locked operation of the fiber laser. The measured auto-correlation trace of laser output pulses is shown in Fig. 4(d). Assuming a Gaussian pulse, the full-width half-maximum (FWHM) was estimated at 12.7 ps. In order to exam pulse quality, we compressed the pulse after taping 15% of laser output power. The

#217567 - $15.00 USD Received 22 Jul 2014; revised 6 Sep 2014; accepted 8 Sep 2014; published 11 Sep 2014

laser output pulse was compressed by using an additional delay (60 m) of the conventional SMF-28e fiber, achieving minimum pulse duration of 369 fs, as shown in the inset of the Fig. 4(d).

We also studied the device performance of the fabricated SWCNT-SA at a higher power level. Figure 5(a) shows a microscopic image of the SWCNT-SA surface, demonstrating that the SWCNT/PMMA film is uniformly coated on the side-polished surface of the fiber without significant defects or cracks. To investigate the performance of the SA at higher power, a fiber pulse laser with a double-clad gain fiber was fabricated, including the SWCNT-SA. We observed that degradation of the laser performance, such as unstable pulsating or decrease of laser output power, started at an average power of about 1 W in the SA. This corresponds to a saturation fluence of 97 mJ/cm^2 per pulse where the saturation fluence was calculated for the mode-field area of core-mode in an optical fiber. It should be noted that this is a much larger value than those in previous results (~100 μJ/cm^2) for fiber-ferrule-type SWCNTs [21]. This enhanced damage threshold in our device is mainly due to the lateral interaction scheme that evanescently interacts with the well-dispersed SWCNT/PMMA composite. After exposing the SA to high powers, we observed visible surface damage along the fiber core on the surface of the SWCNT/PMMA film, as shown in Fig. 5(b). The insertion loss of the SA drastically increases to – 30 dB, which might be due to optical scattering losses and coupling to leakage modes in the side-polished section.

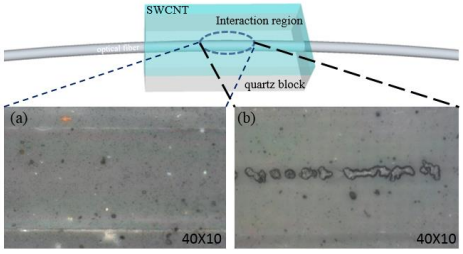

Fig. 5. Microscope image of (a) SWCNT/PMMA composite uniformly coated on the SPF, and (b) visible defects in the SWCNT/PMMA film along the fiber core after exposure to high power.

4. Conclusions

In summary, we fabricated an SPF-based SWCNT-SA for high-power operation of mode-locked fiber lasers. The fabricated SWCNT-SA exhibits reduced insertion loss and polarization-dependent loss compared to previous work. An all-fiber dissipative soliton laser oscillator including the fabricated SWCNT-SA was demonstrated, which delivers a linearly chirped pulse with a pulse energy of 34 nJ at the fundamental repetition rate of 9.80 MHz. The spectral bandwidth and the pulse duration at laser output were measured as 12.1 nm and 12.7 ps, respectively. We also studied the damage threshold of the fabricated SWCNT-SA on an SPF for the first time. We found that visible surface damage developed above the saturation fluence of 97 mJ/cm^2, which is much higher than that of fiber-ferrule-type SA. We expect that our fiber laser can be applied to simplify chirped pulse amplification (CPA) systems for realizing compact ultrafast fiber laser systems with high pulse energy.

Acknowledgments

This research was supported by NRF of Korea (NRF-2013R1A1A2A10005230) funded by MEST and by the Pioneer Research Center Program through the NRF of Korea funded by the Ministry of Science, ICT & Future planning (2011-0027920). S. Y. Choi and F. Rotermund have been supported by NRF of Korea (2011-0017494).